Application of HPLC Combined with UPLC–Orbitrap–MS in Chemical Characterization, Quantitative Detection, and Species Authentication of Four Panax-derived Products

Xingwang Leng
Hunan University of Chinese Medicine
Sicheng Wang
Zhejiang University
Anqi Wang
Hunan University of Chinese Medicine
Bin Li
Hunan University of Chinese Medicine
Lidong Cheng
Hunan Yirentang Chinese Herbal Pieces Co., Ltd.
Yixing Qiu
Hunan University of Chinese Medicine
Jisheng Liu
Hunan University of Chinese Medicine
Jiao Cui
The Second Affiliated Hospital of Hunan University of Chinese Medicine
Xiaoping Nie
The Second Affiliated Hospital of Hunan University of Chinese Medicine
Wei Wang
Hunan University of Chinese Medicine
Xueli Bai
Zhejiang University
Hanwen Yuan
Hunan University of Chinese Medicine
Caiyun Peng
Caiyunpeng@hnucm.edu.cn
Hunan University of Chinese Medicine

Research Article

Keywords: ginsenosides, Panax, HPLC, LC-Orbitrap-MS

Posted Date: October 20th, 2025

DOI: https://doi.org/10.21203/rs.3.rs-7772424/v1

Additional Declarations: No competing interests reported.

Version of Record: A version of this preprint was published at Chromatographia on December 18th, 2025. See the published version at https://doi.org/10.1007/s10337-025-04468-7.

Abstract

Panax species are medicinal plants of high pharmaceutical and economic value. However, the high degree of similarity in their chemical compositions often leads to issues of adulteration and challenges in quality control. This study developed an integrated analytical strategy combining high-performance liquid chromatography (HPLC) and ultra-performance liquid chromatography–Orbitrap mass spectrometry (UPLC–Orbitrap–MS) to systematically characterize and differentiate four major Panax species: Panax ginseng (RS), Panax quinquefolius (XYS), Panax notoginseng (SQ), and Panax japonicus (BSQ). The established HPLC method proved robust and reliable, enabling the simultaneous quantification of 13 bioactive compounds, including 11 saponins and 2 polyacetylenes, and demonstrated excellent precision, reproducibility, and accuracy. The approach clearly revealed content variations of major constituents among the different species. Chemical fingerprinting combined with similarity analysis indicated significant interspecies differences. A total of 129 compounds were identified using high-resolution mass spectrometry, covering structure types such as protopanaxadiol-type, protopanaxatriol-type, oleanane-type, ocotillol-type, and C-17 side-chain variant saponins. By elucidating the characteristic fragmentation patterns of representative ginsenosides, this work offered a theoretical foundation for reliable compound identification. The results provided a scientific foundation for quality assessment and species authentication, offering a comprehensive strategy for the standardization of Panax-derived medicinal products.

1. Introduction

Plants of the Panax species represent a pharmaceutically significant group with demonstrated therapeutic benefits in human health[1]. Although the roots of P. ginseng (RS), P. quinquefolius (XYS), P. notoginseng (SQ), and P. japonicus (BSQ), share close genetic relationships and contain similar bioactive compounds, they exhibit distinct properties, flavors, and clinical applications. Different Panax species vary in their traditional Chinese medicine (TCM) nature and core functional properties. RS (warm nature) is well-recognized for its adaptogenic and energy-enhancing effects[2–4]. BSQ (mildly warm) exerts extensive antioxidant, immunomodulatory, and cardioprotective activities[5]. XYS (cool nature) shows efficacy in anti-fatigue and anti-anxiety applications[6]. SQ (warm nature) is mainly used for its haemostatic and circulatory benefits[7].

These four herbal materials are among the most widely used medicinal plants globally and hold significant shares in the natural product market. Growing demand has highlighted differences in their pharmacological effects, indications, and clinical uses, leading to varying medicinal and economic values[8]. However, their similar chemical profiles have led to widespread issues of adulteration, substitution, and counterfeit products in the market, particularly in powdered formulations and raw materials for proprietary medicines[9]. For instance, XYS is sometimes adulterated into RS products to reduce costs, and the roots of P. vietnamensis are often mistakenly or intentionally used in place of SQ[10–12]. Such practices compromised therapeutic outcomes and raised safety concerns, damaging the credibility of the herbal supply chain. Thus, there is an urgent need to develop accurate species identification methods and investigate the relationship between chemical composition and quality to ensure efficacy, safety, and market standardization.

The establishment of rapid and reliable identification methods and quality assessment protocols for these four Panax species is imperative. Recent advances in analytical techniques have enabled various effective strategies. Chromatographic methods, including high-performance liquid chromatography (HPLC) and ultra-performance liquid chromatography (UPLC), coupled with mass spectrometry (LC–MS) and chemometrics, have shown great promise in the compositional analysis of Panax plants[13–15]. Notably, the integration of chromatographic fingerprinting with high-resolution mass spectrometry (MS) and chemometric analyses, such as principal component analysis (PCA) and orthogonal projection to latent structures–discriminant analysis (OPLS-DA), markedly improves the scientific rigor and reliability of the results[16]. This combined approach facilitates a transition from single-compound quantification toward holistic quality assessment and enables deeper mechanistic insights into the pharmacological properties of phytochemical compositions.

To address quality control and species authentication challenges of Panax-derived products, this study validated an HPLC method for simultaneous quantification of 11 major ginsenosides and 2 polyacetylenes, identified saponins and clarified their fragmentation pathways in four Panax species via high-resolution LC-MS, and screened potential quality markers through chemometric modeling. This work thus holds significance in establishing a more scientific and comprehensive quality evaluation system for Panax plants, a development that aids in resolving quality control and species authentication issues of Panax-derived medicinal products.

2. Materials and Methods

2.1 Reagents and Chemicals

Methanol and acetonitrile of HPLC grade were sourced from Sigma–Aldrich (St. Louis, USA). Other reagents were procured through the China National Medicines Group Chemical Reagent Co., Ltd. (Shanghai, China). Purified water for all aqueous solutions was supplied by China Resources C'estbon Beverage Co., Ltd. (Shenzhen, China). The Nylon filter (0.22 μm, 13 mm in diameter) was supplied by Hangzhou Special Paper Industry Co., Ltd. (Hangzhou, China). The reference standards, including notoginsenoside R1, ginsenoside Rg1, ginsenoside Re, ginsenoside Rb1, ginsenoside Ro, ginsenoside Rc, ginsenoside Rb2, ginsenoside Rb3, chikusetsusaponin IV, ginsenoside Rd, chikusetsusaponin IVa, panaxydol, and panaxynol, were obtained from Shanghai Yuanye Bio-Technology Co., Ltd. (Shanghai, China). A purity level of over 98% was determined for all reference standards by HPLC analysis.

2.2 Plant Materia

A total of 41 medicinal material batches, including 11 batches of BSQ, 10 batches of SQ, 10 batches of XYS, and 10 batches of RS, were collected from Hunan, Hubei, Yunnan, and Jilin provinces in China, as well as Canada and other regions (Table S1). Professor Wei Wang from the School of Pharmacy at Hunan University of Chinese Medicine has authenticated all the materials, which are now stored in the TCM and Ethnomedicine Innovation & Development International Laboratory.

2.3 Preparation of Sample and Standard Solution

Accurately weighed 1.0 g of powdered sample (passed through a No. 5 sieve) was placed in a stopper-sealed conical flask. Exactly 25 mL of methanol was added, and the total weight was recorded. After ultrasonication (30 min) and cooling to room temperature, the weight was measured again, with any solvent loss compensated by adding methanol. The mixture was vortexed, filtered, and the resulting filtrate was further passed through a 0.22 μm microporous membrane to obtain the final test solution for analysis. Accurately weighed appropriate amounts of the reference standards were separately placed in 5 mL volumetric flasks and dissolved in methanol to prepare stock solutions. These stock solutions were diluted to an appropriate multiple and then used for analysis.

2.4 HPLC analysis

The analysis was performed using an Agilent 1260 Infinity II series high-performance liquid chromatography (HPLC) system (Agilent Technologies, Santa Clara, CA, USA), equipped with a binary pump, an autosampler, a thermostatted column compartment, and a diode array detector. Elution was carried out using a gradient program with acetonitrile (A) and 0.1% phosphoric acid in water (B) as the mobile phase at a flow rate of 1 mL/min as follows: 0–20 min, 20–20% A; 20–60 min, 20–40% A; 60–70 min, 40–60% A; 70–75 min, 60–73% A; 75–90 min, 73–95% A; 90–100 min, 95% A. The detection wavelength was set at 203 nm. Both the column and sample compartment temperatures were maintained at 24°C. The injection volume was 5 μL. Separation was achieved using an Agilent Eclipse XDB-C18 column (4.6 mm × 250 mm, 5 μm).

For precision evaluation, the identical sample was injected 6 times consecutively. The sample's stability was determined by conducting analyses at intervals of 0, 4, 8, 12, 24, and 48 h. Reproducibility was tested by preparing 6 parallel samples. Data regarding the retention times and peak areas of corresponding peaks, along with the relative standard deviations for the retention and peak areas of 11 saponins and 2 polyacetylenes, were both logged and computed. Recovery was assessed by spiking at high, medium, and low amounts of standards into weighed samples by 3 replicates, and analyzed by the HPLC method. Recovery was calculated according to the following equation:

Recovery (%) = measure amount − original amount spiked amount × 100%.

2.5 LC–MS Conditions

Chromatography was conducted on a Hypersil GOLD™ Aq-C18 column (100 mm × 2.1 mm, 1.9 μm) using a Vanquish™ Flex UPLC system at 25℃. The elution utilized a gradient of acetonitrile (A) and 0.1% formic acid in water (B) at 0.3 mL/min: 0–10 min, 20 ~ 20% A; 10–45 min, 20–40% A; 45–50 min, 40–60% A; 50–60 min, 60–95% A; 60–75 min, 95% A. The sample compartment temperature was maintained at 25℃, and the injection volume was 4 μL. The ESI-equipped Orbitrap Exploris 120 mass spectrometer functioned in negative polarity modes, conducting both full scan and data-dependent MS/MS (Full MS/ddMS2) analyses with parameters finely tuned for optimal performance. For MS1, the positive mode was set at a spray voltage of 3500 V, while the negative mode was at 2500 V. The gas flow for sheath, auxiliary, and sweep gases were tuned to 50, 10, and 0 Arb, respectively. Meanwhile, the temperatures for the ion transfer tube and vaporizer were stabilized at 325℃ and 350℃, respectively. A resolution of 60,000 and a scanning range of 100–1300 Da were utilized. The HCD Collision Energy for dd-MS2 was set to 30% and the resolution was adjusted to 15,000.

2.6 Data Analysis

Similarity analysis was performed using the "Similarity Evaluation System for Chromatographic Fingerprint of Traditional Chinese Medicine (2002A)". The cosine similarity algorithm was applied to calculate the similarity between chromatographic profiles, enabling a comprehensive evaluation of the overall consistency of chromatographic patterns across different samples. Mass spectrometry data were subjected to raw data preprocessing and format conversion using Freestyle 1.8 software under the Thermo Fisher Scientific platform. PCA and OPLS-DA models were analyzed using SIMCA 14.1 software.

3. Results and Discussion

3.1 HPLC fingerprint

The HPLC analytical method established in this study achieved satisfactory separation for 13 characteristic components, including notogisenoside R1, ginsenoside Rg1, ginsenoside Re, ginsenoside Rb1, ginsenoside Ro, ginsenoside Rc, ginsenoside Rb2, ginsenoside Rb3, chikusetsusaponin IV, ginsenoside Rd, chikusetsusaponin IVa, panaxydol, and panaxynol, which were unequivocally identified through comparison with reference standards (Fig. 1). Among them, ginsenoside Rg1, Re, Rb1, Rd, panaxydol, and panaxynol were identified as common constituents shared by all four medicinal materials.

Method validation results (Tables S2-S7) confirmed the excellent performance of the developed method, with precision (RSD 0.01%-1.23%), repeatability (RSD 0.05%-2.15%), stability (RSD 0.12%-3.45% over 24 h), and robustness (RSD 0.15%-4.11%) all meeting the requirements specified in the Chinese Pharmacopoeia (2020 edition). These findings verify the method's reliability and suitability for quality control of Panax medicinal materials.

The acquired chromatograms were imported in AIA file format into the "Similarity Evaluation System for Chromatographic Fingerprint of Traditional Chinese Medicine (2004A)" for similarity analysis. Characteristic fingerprints were successfully established for XYS (Fig. S1), RS (Fig. S2), SQ (Fig. S3), and BSQ (Fig. S4), with similarity ranges of 0.905–0.987, 0.910–0.966, 0.923–0.991, and 0.911–0.983, respectively. The intra-species similarities of all fingerprints exceeded 0.905, demonstrating good reproducibility and strong specificity of the analytical method. Detailed sample information and similarity data are provided in Tables S7–S10.

Using the characteristic fingerprint of XYS as a reference, a common pattern fingerprint (Fig. S5) was generated by comparison with the 3 other medicinal materials. The results revealed that the similarities between BSQ and RS, SQ, and XYS were all below 0.203, indicating significant differences in their chemical compositions. In contrast, the similarity between RS and XYS approached 0.9, reflecting a high degree of chemical consistency between these two

species. This observation aligned with their shared phylogenetic classification within the Panax medicinal materials and their similar ginsenoside-rich phytochemical profiles, which also accounted for the frequent substitution and confusion between these two species in the commercial market.

3.2 Contents of 11 saponins and 2 polyacetylenes

The recovery rates for 11 saponins and 2 polyacetylenes ranged from 97.49% to 107.32%, with relative standard deviations (RSDs) between 0.99% and 4.54% (Table S8), demonstrating that the method exhibits good sensitivity and accuracy for the detection of saponins and polyacetylenes in Panax species. The linearity of the method was assessed by analyzing 6 standard solutions of different concentrations, and the limits of detection (LOD) and quantification (LOQ) were established using signal-to-noise (S/N) ratios of 3 and 10, respectively (Table 1).

Table 1
Calibration curves, linear ranges, LOD, and LOQ of the analytes.

Analytes	Calibration curves	R^2	Linear range (mg/mL)
Notoginsenoside R1	y = 1482.2x + 3.2034	0.9998	0.07 ~ 0.45
Ginsenoside Rg1	y = 1639x + 21.444	0.9991	0.018 ~ 1.71
Ginsenoside Re	y = 1226x + 8.0829	0.9992	0.01 ~ 0.92
Ginsenoside Rb1	y = 1167.9x + 62.751	0.9998	0.03 ~ 1.94
Ginsenoside Ro	y = 1691.9x + 92.014	1	0.01 ~ 0.43
Ginsenoside Rc	y = 825.47x + 2.5608	0.9996	0.09 ~ 2.8
Ginsenoside Rb2	y = 917.53x + 2.3707	0.9996	0.003 ~ 0.22
Ginsenoside Rb3	y = 883.95x + 1.4466	0.9995	0.006 ~ 0.18
Chikusetsusaponin IV	y = 1735.5x + 20.492	0.9991	0.02 ~ 1.68
Ginsenoside Rd	y = 1491x + 3.5923	0.9999	0.01 ~ 0.45
Chikusetsusaponin IVa	y = 1741.4x + 11.189	0.9991	0.01 ~ 0.82
Panaxydol	y = 5183.6x + 6.8628	0.9996	0.1125 ~ 0.16
Panaxynol	y = 12488x + 229.58	0.9996	0.002 ~ 0.12

This study employed standard curves for content determination. The significant differences in chemical composition among the four medicinal materials were evident from their respective content chromatograms (Fig. 3). SQ was uniquely characterized by a high level of notoginsenoside R1 (6.33–9.30 mg/g), which serves as a specific chemical marker for its identification. BSQ exhibited a distinct chemical profile dominated by exceptionally high concentrations of ginsenoside Ro (68.17–128.57 mg/g) along with significant amounts of chikusetsusaponin IV and IVa, clearly distinguishing it from other species. Although XYS and RS share a similar set of ginsenosides (e.g., Rc, Rb2, Rb3), they can be effectively differentiated by their characteristic ginsenoside Re/Rb1 ratio. XYS showed notably higher levels of ginsenoside Re (7.64–23.44 mg/g), while RS displayed a more balanced distribution of protopanaxadiol- and protopanaxatriol-type ginsenosides.

3.3 LC–MS Analysis

The total ion chromatograms (TICs) of the four materials obtained by LC–Orbitrap-MS are presented in Fig. 4. Data processing, including blank subtraction, deconvolution, peak extraction, and database searching against spectral libraries (mzCloud, mzVault) and a self-built database, was performed using Compound Discoverer. Compounds were initially filtered using thresholds of an mzCloud Best Match score ≥ 80 and mzCloud Best Match confidence ≥ 80, or an mzVault Best Match score ≥ 80. To minimize false positives, constituents with low spectral reliability, such as those exhibiting poor fragmentation or low intensity in MS^2 spectra, were excluded. The identification accuracy was further improved by requiring a minimum number of matched product ions. A targeted screening approach was enhanced by incorporating literature-derived MS^1 and MS^2 data on known compounds in these four Panax species. A total of 129 compounds were identified across the four species. Specifically, 81, 78, 83, and 85 compounds were detected in BSQ, RS, SQ, and XYS, respectively. These included 34 protopanaxadiol-type saponins, 26 protopanaxatriol-type saponins, 17 C-17 side-chain varied saponins, 14 oleanane-type saponins, 8 ocotillol-type saponins, and 64 other compounds, as summarized in Table 2. Representative MS^2 spectra of selected compounds are provided in Fig. S6.

Table 2
The compounds identified by LC-MS.

NO.	RT [min]	Identification	Formula	Diff. [ppm]	m/z	Reference Ion	Fragments Ions (m/z)	BSC
1	1.25	Vinaginsenoside R4	$C_{47}H_{80}O_{19}$	-1.58	993.5292	[M + COOH]-	947.5223,785.4705,767.4596, 635.4165	√
2	1.34	Floralquinquenoside D	$C_{42}H_{72}O_{15}$	-1.03	861.4862	[M + COOH]-	653.4216, 491.3742, 391.2861	√
3	1.61	Yesanchinoside B	$C_{48}H_{82}O_{20}$	1.12	1023.5393	[M + COOH]-	977.5334,815.4803,653.4267, 491.3742	√
4	2.17	Ginsenoside Re5 isomer/ Ginsenjilinol isomer	$C_{42}H_{72}O_{15}$	-1.38	861.4865	[M + COOH]-	815.4778,653.4274,491.3739	√
5	2.35	Vinaginsenoside R4/ Majonoside F5	$C_{48}H_{82}O_{19}$	1.15	1007.5444	[M + COOH]-	961.5388, 815.4813,799.4864, 653.4271, 491.3731	
6	2.58	Ginsenoside Re5 isomer/ Ginsenjilinol isomer	$C_{42}H_{72}O_{15}$	3.08	861.4879	[M + COOH]-	815.4824,653.4316,491.3760	√
7	2.95	Floralginsenoside P isomer	$C_{53}H_{90}O_{23}$	1.12	1093.5804	[M-H]-	961.5385,799.4838,637.4329, 475.3789	
8	3.72	Majonoside R1	$C_{42}H_{72}O_{15}$	0.79	861.4861	[M + COOH]-	815.4807,653.4271,591.3742, 391.2851	√
9	3.76	Ginsenoside Re1/Re2/Re3	$C_{48}H_{82}O_{19}$	1.21	1007.5445	[M + COOH]-	961.5393, 799.4906,637.4330, 475.3797	√
10	5.17	Yesanchinoside E	$C_{54}H_{92}O_{23}$	0.76	1153.6023	[M + COOH]-	1107.5961,961.5403,783.4889, 637.4313,475.3794	
11	5.63	Quinquenoside F6	$C_{47}H_{80}O_{18}$	1.30	977.5340	[M + COOH]-	931.5258,799.4898,637.4323, 475.3809	
12	6.83	Ginsenoside Re4	$C_{47}H_{80}O_{18}$	-1.58	977.5342	[M + COOH]-	931.5295,799.4946,637.4330, 475.3756	
13	7.07	Ginsenoside Rg1 isomer	$C_{42}H_{72}O_{14}$	-1.35	845.4916	[M + COOH]-	799.4857,653.4272,491.3740, 391.2848	√
14	7.27	Notoginsenoside N/M	$C_{48}H_{82}O_{19}$	1.17	961.5375	[M-H]-	799.4866, 637.4327, 475.3786	
15	7.39	Notoginsenoside R1[a]	$C_{47}H_{80}O_{18}$	-0.99	977.5336	[M + COOH]-	931.5287, 799.4870,769.4736, 637.4327, 475.3797	√
16	8.74	Ginsenoside Re isomer	$C_{48}H_{82}O_{18}$	-2.00	991.5503	[M + COOH]-	945.5449,783.4927,637.4338, 475.3811	
17	9.11	Notoginsenoside ST5	$C_{47}H_{80}O_{18}$	1.58	977.5342	[M + COOH]-	931.5308,799.4885,637.4332, 475.3801	
18	9.72	Quinquenoside IV	$C_{54}H_{90}O_{24}$	1.27	1167.5821	[M + COOH]-	1121.5747,959.5238,797.4669,	
19	10.57	Ginsenoside Rg1 isomer	$C_{42}H_{72}O_{14}$	0.02	845.4904	[M + COOH]-	815.0154, 799.4916,637.4333, 475.3786	√
20	10.57	Ginsenoside Rg1[a]	$C_{42}H_{72}O_{14}$	-0.77	845.4911	[M + COOH]-	799.4871, 637.4330,475.3794,	√
21	11.59	Ginsenoside Re[a]	$C_{48}H_{82}O_{18}$	-1.09	991.5494	[M + COOH]-	945.5438, 783.4899,637.4331, 475.3796	√
22	13.86	Ginsenoside Rg1 isomer	$C_{42}H_{72}O_{14}$	-1.41	845.4916	[M + COOH]-	799.4854,653.4271,491.3740	√
23	17.37	Malonylginsenoside Rg1	$C_{45}H_{74}O_{17}$	1.42	885.4866	[M-H]-	637.4338,619.4233,475.3789	

NO.	RT [min]	Identification	Formula	Diff. [ppm]	m/z	Reference Ion	Fragments Ions (m/z)	BSC
24	17.58	Vinaginsenoside R13	$C_{48}H_{84}O_{20}$	1.53	979.5468	[M-H]-	817.4965, 799.4860,655.4434, 637.4316	
25	18.09	Malonylginsenoside Rf	$C_{45}H_{74}O_{17}$	1.52	885.4867	[M-H]-	799.4896,637.4344,619.4215, 475.3811	
26	19.34	Malonylginsenoside Re	$C_{51}H_{84}O_{21}$	0.86	1031.5441	[M-H]-	945.5436, 783.4910,637.4319, 475.3790	√
27	19.34	Acetyl ginsenoside Re	$C_{50}H_{84}O_{19}$	0.49	987.5539	[M-H]-	945.5434,783.4904,637.4319, 475.3792	
28	19.74	Acetyl notoginsenoside R1	$C_{50}H_{84}O_{21}$	2.00	1019.5453	[M-H]-	931.5303,799.4892,637.4332, 619.4190,475.3795	
29	22.16	B1-20-Glc-Glc-6-Glc-Glc	$C_{54}H_{94}O_{24}$	1.77	1171.6138	[M + COOH]-	1125.6068,963.5540,801.5015, 783.4926	
30	22.49	Pseudoginsenoside Rt2	$C_{41}H_{70}O_{14}$	-1.81	831.4763	[M + COOH]-	785.4711,653.4276,491.3740	√
31	22.64	PseudoginsenosideRC1	$C_{50}H_{84}O_{19}$	1.47	1033.5604	[M + COOH]-	945.5449,783.4912,637.4331, 475.3793	√
32	23.11	Majonoside R2	$C_{41}H_{70}O_{14}$	1.03	831.4757	[M + COOH]-	785.4705,653.4280,491.3750	√
33	23.27	Pseudoginsenoside Rt	$C_{36}H_{62}O_{10}$	-1.07	699.4333	[M + COOH]-	653.4262,491.3764	√
34	23.94	Ginsenoside Rf isomer	$C_{42}H_{72}O_{14}$	-1.62	845.4918	[M-H]-	799.4851,637.4342,619.4222, 475.3797	√
35	24.36	Quinquenoside L11	$C_{42}H_{72}O_{14}$	-0.90	845.4912	[M + COOH]-	799.4858, 653.4275,491.3739,	√
36	24.36	Pseudoginsenoside F11	$C_{42}H_{72}O_{14}$	-6.97	799.4794	[M + COOH]-	653.4275,491.3746,415.3222	√
37	25.23	24(R)-pseudoginsenoside F11	$C_{42}H_{72}O_{14}$	0.31	799.4832	[M-H]-	637.4327, 475.3780	√
38	25.77	Quinquenoside L6	$C_{48}H_{80}O_{18}$	1.48	989.5342	[M + COOH]-	943.5281781.4752,619.4212	√
39	25.84	Ginsenoside Rf isomer	$C_{42}H_{72}O_{14}$	-1.61	845.4918	[M + COOH]-	799.4862, 637.4318, 475.3782	√
40	26.42	Ginsenoside Rf[a]	$C_{42}H_{72}O_{14}$	1.19	845.4914	[M + COOH]-	799.4896, 637.4313, 475.3786	
41	26.43	Ginsenoside Rf isomer	$C_{42}H_{72}O_{14}$	-1.21	845.4914	[M + COOH]-	799.4861,637.4318,475.3787	√
42	27.01	Ginsenoside F5	$C_{41}H_{70}O_{13}$	0.73	815.4806	[M + COOH]-	769.4750, 637.4322, 475.3793	√
43	27.87	Ginsenoside Rf isomer	$C_{42}H_{72}O_{14}$	-1.53	845.4917	[M + COOH]-	799.4960,637.4305,475.3822	√
44	28.55	Ginsenoside Rg2 isomer	$C_{42}H_{72}O_{13}$	1.04	829.4965	[M + COOH]-	783.4905,637.4332,475.3794	
45	28.59	Ginsenoside F3	$C_{41}H_{70}O_{13}$	-1.42	815.4810	[M + COOH]-	637.4305,475.3792	
46	28.74	20(S)-Ginsenoside Rh1[a]	$C_{36}H_{62}O_{9}$	-0.48	683.4379	[M + COOH]-	637.4282,475.3793	√
47	29.24	Ginsenoside Rg2[a]	$C_{42}H_{72}O_{13}$	-1.00	829.4963	[M + COOH]-	783.4911, 637.4327, 475.3796	√
48	29.38	Ginsenoside Ra3	$C_{59}H_{100}O_{27}$	0.47	1285.6428	[M + COOH]-	1107.5964,945.5447,783.4913, 621.4388	√
49	29.38	Notoginsenoside R4	$C_{59}H_{100}O_{27}$	-0.58	1285.6430	[M + COOH]-	1239.6398,1107.5957,1077.5864,945.5438,783.4894	

NO.	RT [min]	Identification	Formula	Diff. [ppm]	m/z	Reference Ion	Fragments Ions (m/z)	BSC
50	29.68	notoginsenoside R2	$C_{41}H_{70}O_{13}$	-1.75	815.4813	[M + COOH]-	769.4719, 637.4291, 475.3798	
51	29.70	20(R)-Ginsenoside Rh1	$C_{36}H_{62}O_{9}$	-1.27	683.4385	[M + COOH]-	637.4349, 475.3799	√
52	30.64	Notoginsenoside Fa	$C_{59}H_{100}O_{27}$	0.04	1285.6434	[M + COOH]-	1107.5964,945.5482,783.4912, 621.4382, 459.3853	√
53	30.65	Ginsenoside Ro isomer	$C_{48}H_{76}O_{19}$	1.25	955.4920	[M-H]-	793.4400,731.4383,631.3849, 567.3701	√
54	30.79	Malony notoginoside R4	$C_{62}H_{102}O_{30}$	-0.26	1325.6380	[M-H]-	1239.6392,1107.5951,945.5432,783.4902,621.4391	
55	31.02	Ginsenoside Ro isomer	$C_{48}H_{76}O_{19}$	1.22	955.4920	[M-H]-	793.4360, 631.3850, 455.3521	√
56	31.19	Ginsenoside Rh7	$C_{36}H_{60}O_{9}$	-0.89	681.4225	[M + COOH]-	635.4201,473.3641	√
57	31.25	Notoginsenoside I	$C_{54}H_{92}O_{22}$	0.95	1091.6011	[M-H]-	1091.6027, 929.5491,767.4955, 605.4443	√
58	31.42	Ginsenoside Ro isomer	$C_{48}H_{76}O_{19}$	1.12	955.4919	[M-H]-	793.4396, 731.4379, 613.3751, 569.3850	√
59	31.99	5,6-Dihydroginsenoside Rb1	$C_{54}H_{90}O_{23}$	1.19	1105.5802	[M-H]-	943.5283, 781.4746, 619.4221, 457.3685	√
60	32.03	Ginsenoside Ro isomer	$C_{48}H_{76}O_{19}$	1.38	955.4921	[M-H]-	793.4406, 731.4396, 631.3869, 569.3854, 523.3801	√
61	32.23	Ginsenoside Rh8	$C_{36}H_{60}O_{9}$	-1.21	681.4228	[M + COOH]-	626.2918,473.3637	√
62	32.38	Ginsenoside Rb1[a]	$C_{54}H_{92}O_{23}$	-0.36	1153.6016	[M + COOH]-	1107.5963,945.5442,783.4905, 621.4370	
63	32.54	Yesanchinoside D/ Vinaginsenoside R1	$C_{44}H_{74}O_{15}$	-0.88	887.5018	[M + COOH]-	841.4966,799.4870,653.4386, 587.3959,491.3762	√
64	32.58	Malonynotoginoside R4 isomer	$C_{62}H_{102}O_{30}$	-0.12	1325.6382	[M-H]-	1239.6395,1107.5956,1089.5851, 945.5433, 783.4905	
65	33.18	Ginsenoside F1	$C_{36}H_{62}O_{9}$	-0.33	683.4378	[M + COOH]-	637.4292,475.3796	√
66	33.51	Ginsenoside Ro isomer	$C_{48}H_{76}O_{19}$	1.59	955.4923	[M-H]-	793.4389,731.4380,	√
67	33.59	Ginsenoside Rc[a]	$C_{53}H_{90}O_{22}$	1.01	1123.5919	[M + COOH]-	945.5450, 783.4906, 621.4368, 459.3876	√
68	33.59	Ginsenoside V	$C_{54}H_{92}O_{24}$	0.23	1123.5908	[M-H]-	1077.5855,945.5249,783.4904, 621.4374,459.3857	√
69	33.73	MalonynotoginosideR4 isomer	$C_{62}H_{102}O_{30}$	-0.41	1325.6378	[M-H]-	1239.6381,1107.5946,945.5421, 783.4898	
70	33.84	Malony ginsenoside Rb1	$C_{57}H_{94}O_{26}$	0.89	1193.5971	[M-H]-	1107.5958, 945.5427,783.4899, 621.4373	√
71	33.97	Ginsenoside Ro[a]	$C_{48}H_{76}O_{19}$	1.29	955.4920	[M-H]-	793.4397, 613.3754, 569.3854, 455.3543	
72	34.24	Malonyginsenoside Rb1 isomer	$C_{57}H_{94}O_{26}$	1.09	1193.5974	[M-H]-	1107.5973,1089.5869,945.5444,783.4910, 621.4377,459.3876	√
73	34.44	Ginsenoside Rs1/ Ginsenoside Rs2	$C_{55}H_{92}O_{23}$	-2.26	1119.5931	[M-H]-	1077.5864,1059.5767,945.5444,783.4908, 765.4805	
74	34.68	Malony ginsenoside Rb1 isomer	$C_{57}H_{94}O_{26}$	1.38	1193.5977	[M-H]-	1107.5973,945.5436,783.4921, 621.4385	√
75	35.23	Chikusetsusaponin Ⅳ	$C_{42}H_{66}O_{14}$	1.27	793.4390	[M-H]-	631.3865, 569.3864, 455.3536	√
76	35.28	Ginsenoside Rb2[a]	$C_{53}H_{90}O_{22}$	-1.26	1123.5920	[M + COOH]-	1077.5863, 945.5488,783.4912, 621.4350, 459.3821	

NO.	RT [min]	Identification	Formula	Diff. [ppm]	m/z	Reference Ion	Fragments Ions (m/z)	BSC
77	35.46	Malonyl ginsenoside Ro	$C_{51}H_{78}O_{22}$	0.23	1041.4931	[M-H]-	997.5026,937.4821,835.4489, 775.4276,731.4383	
78	35.56	Malony ginsenoside Rb1 isomer	$C_{57}H_{94}O_{26}$	5.41	1193.5896	[M + COOH]-	1107.5968,1078.5889,945.5440,783.4877,621.4351	√
79	35.56	Isomeric Ginsenoside V	$C_{54}H_{92}O_{24}$	-1.36	1123.5921	[M + COOH]-	1077.5857,945.5440,915.5322, 783.4895,621.4367	
80	35.60	Malony ginsenoside Rb1 isomer	$C_{57}H_{94}O_{26}$	-7.04	1193.5877	[M-H]-	1107.5960,1078.5892,945.5432,783.4895,621.4338	
81	35.64	Malonyl ginsenoside Ro isomer	$C_{51}H_{78}O_{22}$	1.63	1041.4929	[M-H]-	997.50305,835.4504,773.4487, 613.3742,569.3854	
82	35.75	Pseudoginsenoside RT1[a]	$C_{47}H_{74}O_{18}$	1.32	925.4815	[M-H]-	763.4280, 613.3746, 569.3858	
83	35.85	Ginsenoside Rb3[a]	$C_{53}H_{90}O_{22}$	-0.69	1123.5914	[M + COOH]-	1077.5866, 945.5435,783.4907, 621.4376, 459.3900	√
84	36.03	Chikusetsusaponin IV[a]	$C_{47}H_{74}O_{18}$	0.97	925.4811	[M-H]-	793.4382, 613.3750, 569.3852, 455.3536	√
85	36.28	PPT-Glc-Ace	$C_{38}H_{64}O_{10}$	1.19	725.4490	[M + COOH]-	637.4321,475.3799	
86	36.74	Quinquenoside R1	$C_{56}H_{94}O_{24}$	-0.96	1195.6129	[M + COOH]-	1107.5967,1089.5863,945.5443,783.4913, 621.4382, 459.3855	√
87	36.83	Malonyl ginsenoside Rb3	$C_{56}H_{92}O_{25}$	1.04	1163.5867	[M-H]-	1077.5864, 945.4912,765.4815, 621.4384, 459.3872	
88	37.32	Chikusetsu saponin IVa[a]	$C_{42}H_{66}O_{14}$	1.22	793.4390	[M-H]-	631.3861, 569.3861, 455.3511	√
89	37.60	Yesanchinoside F	$C_{56}H_{94}O_{24}$	0.35	1195.6120	[M + COOH]-	1107.5969,1089.5864,945.5446,783.4912,621.4384	
90	37.85	Malonyl ginsenoside Rb2	$C_{56}H_{92}O_{25}$	0.27	1163.5858	[M-H]-	1077.5851, 945.5427, 783.4897	√
91	37.93	Ginsenoside Rg8/Rg9	$C_{42}H_{70}O_{13}$	1.41	827.4811	[M + COOH]-	781.4754, 619.4219, 457.3698	√
92	38.01	Chikusetsusaponin IVa isomer	$C_{42}H_{66}O_{14}$	1.40	793.4391	[M-H]-	631.3853, 569.3845, 455.3561	√
93	38.38	Malonyl ginsenoside Rc	$C_{56}H_{92}O_{25}$	2.40	1163.5867	[M-H]-	1077.5867,945.5447,783.4909, 621.4376	√
94	38.48	Acetyl ginsenoside Rd	$C_{50}H_{84}O_{19}$	-2.68	987.5508	[M-H]-	945.5446,783.4912,621.4378, 459.3848	√
95	38.48	Malonyl ginsenoside Rd isomer	$C_{51}H_{84}O_{21}$	1.40	1031.5447	[M-H]-	987.5585,945.5449,783.4917, 621.4385,459.3840	√
96	39.17	Notoginsenoside K	$C_{48}H_{82}O_{18}$	-1.73	991.5500	[M + COOH]-	945.5437,783.4903,621.4375, 459.3861	√
97	39.24	Acetyl ginsenoside Rd isomer	$C_{50}H_{84}O_{19}$	0.73	987.5552	[M-H]-	945.5456,783.4921,765.4807, 621.4385	
98	39.42	Malonyl ginsenoside Rd isomer	$C_{51}H_{84}O_{21}$	1.45	1031.5447	[M-H]-	945.5434, 783.4896, 621.4358	
99	39.53	Acetyl ginsenoside Fc	$C_{55}H_{92}O_{23}$	0.32	1165.6015	[M + COOH]-	1077.58451059.5743,945.5427, 783.4887, 765.4777	
100	39.98	Ginsenoside Rd[a]	$C_{48}H_{82}O_{18}$	-5.00	945.5381	[M-H]-	783.4950, 621.4378, 459.3838	
101	39.99	Gypenoside XVII	$C_{48}H_{82}O_{18}$	1.10	945.5401	[M-H]-	945.5480, 783.4895, 621.4382, 459.3840	√
102	40.28	Quinquenoside □	$C_{50}H_{84}O_{19}$	-1.76	1033.5607	[M + COOH]-	987.5557,945.5457,783.4915, 621.4384,459.3849	√

NO.	RT [min]	Identification	Formula	Diff. [ppm]	m/z	Reference Ion	Fragments Ions (m/z)	BSC
103	40.29	Acetyl ginsenoside Re	$C_{50}H_{84}O_{19}$	1.30	1033.5603	[M + COOH]-	987.5538,945.5444,925.5031, 783.4903,621.4377	√
104	40.30	PPD-Glc-(Glc-Glc)-2malonyl	$C_{54}H_{86}O_{24}$	1.28	1117.5451	[M-H]-	987.5561, 945.5461, 825.5042, 783.4879, 765.4809, 621.4365	√
105	40.48	Acetyl ginsenoside Rd isomer	$C_{50}H_{84}O_{19}$	1.06	987.5543	[M-H]-	945.5440,927.5318,783.4946, 621.4375	
106	40.59	Acetyl ginsenoside Rd isomer	$C_{50}H_{84}O_{19}$	-0.75	987.5529	[M-H]-	945.5447, 783.4916, 621.4379, 459.3849	
107	41.00	Notoginsenoside Fe	$C_{47}H_{80}O_{17}$	1.81	961.5395	[M + COOH]-	915.5329, 753.4825, 621.4378, 459.3850	
108	41.00	Gypenoside XLVI	$C_{48}H_{82}O_{19}$	1.60	961.5393	[M-H]-	915.5339, 753.4791, 621.4377, 459.3860	√
109	41.04	Malonyl ginsenoside Rd isomer	$C_{51}H_{84}O_{21}$	1.56	1031.5448	[M-H]-	945.5442,783.4913,621.4382	√
110	41.91	Malonyl ginsenoside Rd isomer	$C_{51}H_{84}O_{21}$	1.47	1031.5448	[M-H]-	945.5435,783.4941,621.4349	
111	42.17	Malonyl ginsenoside Rd isomer	$C_{51}H_{84}O_{21}$	1.50	1031.5448	[M-H]-	945.5446, 783.4896, 621.4393	
112	42.45	Vinaginsenoside R3	$C_{48}H_{82}O_{17}$	-1.24	975.5546	[M + COOH]-	929.5486,767.4965,605.4433	√
113	42.49	Notoginsenoside Ft1	$C_{47}H_{80}O_{17}$	1.05	915.5293	[M-H]-	783.4911, 621.4381, 459.3839	√
114	43.04	Gypenoside IX	$C_{47}H_{80}O_{17}$	1.79	961.5394	[M + COOH]-	915.5339, 783.4954, 621.4392, 459.3845	√
115	43.65	Gypenoside XLVI isomer	$C_{48}H_{82}O_{19}$	1.27	961.5390	[M-H]-	915.5302, 783.4879, 621.4372, 459.3857	√
116	44.02	Acetyl pseudoginsenside RC1	$C_{52}H_{86}O_{20}$	1.80	1029.5658	[M-H]-	945.5441,927.5289,783.4958, 765.4800,621.4363	√
117	44.28	Ginsenoside F4	$C_{42}H_{70}O_{12}$	2.23	811.4868	[M + COOH]-	765.4805,619.4224,457.3719	
118	46.67	Ginsenoside F2[a]	$C_{42}H_{72}O_{13}$	-0.95	829.4963	[M + COOH]-	783.4917,621.4370,459.3877	√
119	47.16	Chikusetsusaponin Ib	$C_{47}H_{74}O_{18}$	0.91	925.4811	[M-H]-	793.4390, 731.4374, 569.3846, 455.3529	√
120	48.97	20(S)-Ginsenoside Rg3	$C_{42}H_{72}O_{13}$	1.52	829.4967	[M + COOH]-	783.4905, 621.4426, 459.3846	
121	48.98	20(R)-Ginsenoside Rg3[a]	$C_{42}H_{72}O_{13}$	1.52	829.4967	[M + COOH]-	783.4902, 621.4388, 459.3860	
122	49.56	Ginsenoside Rk1	$C_{42}H_{70}O_{12}$	1.94	811.4867	[M + COOH]-	765.4808,603.4275	
123	49.83	Pseudoginsenoside Rp1	$C_{41}H_{64}O_{13}$	0.79	763.4280	[M-H]-	613.3749, 569.3851, 509.3635, 455.3528	√
124	49.92	Ginsenoside Rs5	$C_{44}H_{72}O_{13}$	0.62	807.4906	[M-H]-	765.4796,603.4274	√
125	50.27	Ginsenoside Rs4	$C_{44}H_{72}O_{13}$	1.09	807.4909	[M-H]-	765.4796,603.4257	√
126	51.70	20(S)-Ginsenoside Rh2[a]	$C_{36}H_{62}O_{8}$	-1.06	667.4434	[M + COOH]-	621.4500, 459.3846, 161.0460	√
127	51.92	Ginsenoside Rg5	$C_{42}H_{70}O_{12}$	1.52	765.4783	[M-H]-	603.4280, 441.3755	√
128	52.14	Ginsenoside Rg6	$C_{42}H_{70}O_{12}$	1.33	765.4784	[M-H]-	603.4279, 441.3759	√
129	52.68	Ginsenoside Rh4	$C_{36}H_{60}O_{8}$	-1.13	665.4278	[M + COOH]-	457.3695	√

Note: The superscript letter "a" indicates that the compound was identified by comparison with an authentic reference standard. The check mark (√) indicates that the component was detected in the sample.

In negative-ion mode, the MS1 spectra of protopanaxadiol-type ginsenosides were dominated by the formate adduct $[M + HCOO]^-$ and the deprotonated ion $[M–H]^-$. High-energy collision-induced dissociation (CID) experiments revealed a stepwise loss of sugar substituents, ultimately affording the protopanaxadiol aglycone. Diagnostic fragments appeared at m/z 459.3900. Ginsenoside Rb3 (compound 83) was selected to exemplify the cleavage pattern. It eluted at a retention time (RT) = 35.85 min and exhibited a precursor ion at m/z 1077.5866 ($[M + HCOO]^-$, $C_{53}H_{90}O_{22}$). The MS^2 spectrum displayed sequential losses of one xylose residue ($–C_5H_8O_4$) at m/z 945.5435, one glucose residue ($–C_6H_{10}O_5$) at m/z 783.4907, and two additional glucose units at m/z 621.4376 and 459.3900. These data, together with comparison to the reference standard and literature, unambiguously identified compound 83 as. Its fragmentation pathway is illustrated in Fig. 4a. Similarly, protopanaxatriol-type ginsenosides yield prominent $[M + HCOO]^-$ and $[M–H]^-$ ions. Its MS^2 showed sequential excision of glucose units, termina ginsenoside Rb3ting in the protopanaxatriol aglycone whose characteristic fragments occur at m/z 799.4871, 637.4330, and 475.3794. Ginsenoside Rg1 (compound 21) was eluted at 10.57 min with $[M + HCOO]^-$ at m/z 845.4911 ($C_{42}H_{72}O_{14}$). The spectrum displayed successive losses of two glucose residues ($–C_6H_{10}O_5$) to produce m/z 637.4330 and 475.3794, confirming compound 21 as ginsenoside Rg1 (Fig. 4b). Oleanane-type ginsenosides are also detected as $[M + HCOO]^-$ and $[M–H]^-$ ions. Their sugar moiety is stripped stepwise, delivering the oleanolic acid aglycone (m/z 455). Ginsenoside Ro (compound 71) eluted at 33.97 min with $[M–H]^-$ at m/z 955.4920 ($C_{48}H_{76}O_{19}$). Sequential losses of two glucose units ($–C_6H_{10}O_5$) and one glucuronic acid residue ($–C_6H_8O_6$) generated fragments at m/z 793.4397, 631.4370, and 455.3543, identifying compound 71 as ginsenoside Ro (Fig. 4c). Ocotillol-type ginsenosides also produced abundant $[M + HCOO]^-$ and $[M–H]^-$ ions. Their MS^2 revealed progressive removal of glucose units, yielding the ocotillol aglycone (m/z 491). Majoroside R1 (compound 8) was eluted at 3.72 min ($[M + HCOO]^-$, m/z 861.4861, $C_{42}H_{72}O_{15}$). Stepwise loss of two glucose residues afforded m/z 653.4271 and the diagnostic fragment at m/z 491.3742. Subsequent elimination of C_3H_6O and H_2O produced an additional ocotillol-type ion at m/z 415.3212. These data enabled the identification of compound 8 as majoroside R1 (Fig. 4d). The C-17 side-chain-modified ginsenosides were identified via their representative deprotonated ions ($[M + HCOO]^-$ and $[M–H]^-$) and a characteristic fragment ion at m/z 455. Ginsenoside Rg5 (compound 128) eluted at 51.92 min ($[M–H]^-$, m/z 765.4783). Sequential losses of two glucose units ($–C_6H_{10}O_5$) yielded fragments at m/z 603.4280 and 441.3755, confirming compound 128 as ginsenoside Rg5 (Fig. 4e).

The peak area data of 129 compounds identified by mass spectrometry were imported into SIMCA 14.1 software for principal component analysis (PCA) and orthogonal partial least squares-discriminant analysis (OPLS-DA). The resulting score plots are shown in Fig. 5. Both PCA and OPLS-DA facilitate the visualization of overall clustering trends among samples[17], where the dispersion of points reflects the similarities or differences in composition across samples. In the PCA score plot (Fig. 5A), Panax japonicus and Panax notoginseng were clearly distinguished from Panax ginseng and Panax quinquefolius; however, RS and Panax XYS were not effectively separated, a finding consistent with the chemical fingerprint similarity assessment. In contrast, the supervised OPLS-DA method effectively reduced errors associated with non-experimental factors, yielding more accurate classification results[18]. A 200-permutation test confirmed the model's robustness, with parameters $R^2Y = 0.982$, $R^2X = 0.806$, $Q^2 = 0.964$, and $P < 0.005$, indicating high explanatory and predictive power without overfitting (Figs. 5C and 5D)[19]. Based on a variable importance in projection (VIP) threshold greater than 1.0, 55 differential compounds with contributions were screened, while using a VIP threshold greater than 1.5, 15 significantly contributing differential compounds were identified. The relative abundances of these 15 marker compounds across the four Panax species are visualized in Fig. 6. As shown in Fig. 7, the heatmap visually illustrates the differential relative abundance of 55 ginsenosides across four Panax species. The results demonstrate distinct interspecies clustering, indicating that the accumulation patterns of characteristic ginsenosides were markedly species-specific. Specifically, BSQ was significantly enriched in oleanane-type saponins (e.g., chikusetsusaponin IV and IVa), while SQ was characterized by notoginsenoside R1 and Ft1 as its predominant markers. Although XYS and RS shared certain protopanaxadiol- and protopanaxatriol-type ginsenosides, the former exhibited significantly higher levels of malonylated ginsenosides, further delineating the chemical boundaries between the two species.

4. Conclusion

In this study, an integrated HPLC and UPLC–Orbitrap–MS strategy was successfully established for the comprehensive chemical characterization, quantitative evaluation, and species authentication of four medicinally important Panax medicines. The validated HPLC method permitted the reproducible quantification of 11 major ginsenosides and 2 polyacetylenes in 41 commercial batches. Similarity evaluation of the generated fingerprints revealed high intra-specific consistency and pronounced inter-specific divergence, underscoring the specificity of the approach. Multivariate modelling (PCA/OPLS-DA) delivered unambiguous species segregation; the final OPLS-DA model possessed excellent explanatory and predictive power and afforded clear chemical distinction even between the closely related RS and XYS[20–22]. Heat-map visualisation further demonstrated species-specific accumulation patterns of these markers, underscoring their utility as quality-control indicators. These findings offer a scientific basis for quality assessment, authentication, and standardization of Panax-derived products.

The integrated approach enhanced the capability to detect adulteration and ensure product consistency and supported the development of a more robust quality control system for traditional herbal medicines. Future studies may focus on correlating these chemical markers with pharmacological activities to further validate their roles as quality markers.

Declarations

Author contributions:

Conceptualization, X.L.; methodology, A.W. and L.C.; investigation, X.L. and J.L.; formal analysis, B.L. and J.C.; writing – original draft preparation, S.W. and Y.Q.; writing – review & editing, X.N. and X.B..; project administration, W.W.; supervision, H.Y.; Funding acquisition, C.P. All authors have read and agreed to the published version of the manuscript.

Funding:

This work was supported by the Natural Science Foundation of Hunan Province [Grant No.2024JJ8237, 2023JJ60130, and 2025JJ80144] and National Natural Science Foundation of China (Grant No. 82405012).

Conflicts of Interest:

The authors declare that they have no competing interests.

References

1. Yang, W.Z.; Hu, Y.; Wu, W.Y.; Ye, M.; Guo, D.A. Saponins in the genus Panax L. (Araliaceae): a systematic review of their chemical diversity. *Phytochemistry* **2014**, *106*, 7-24, doi:10.1016/j.phytochem.2014.07.012.
2. Piao, X.; Zhang, H.; Kang, J.P.; Yang, D.U.; Li, Y.; Pang, S.; Jin, Y.; Yang, D.C.; Wang, Y. Advances in Saponin Diversity of Panax ginseng. *Molecules* **2020**, *25*, doi:10.3390/molecules25153452.
3. Ratan, Z.A.; Haidere, M.F.; Hong, Y.H.; Park, S.H.; Lee, J.-O.; Lee, J.; Cho, J.Y. Pharmacological potential of ginseng and its major component ginsenosides. *Journal of Ginseng Research* **2021**, *45*, 199-210, doi:10.1016/j.jgr.2020.02.004.
4. Zhou, G.; Wang, C.Z.; Mohammadi, S.; Sawadogo, W.R.; Ma, Q.; Yuan, C.S. Pharmacological Effects of Ginseng: Multiple Constituents and Multiple Actions on Humans. *Am J Chin Med* **2023**, *51*, 1085-1104, doi:10.1142/s0192415x23500507.
5. Chen, Y.; Liu, M.; Wen, J.; Yang, Z.; Li, G.; Cao, Y.; Sun, L.; Ren, X. Panax japonicus C.A. Meyer: a comprehensive review on botany, phytochemistry, pharmacology, pharmacokinetics and authentication. *Chin Med* **2023**, *18*, 148, doi:10.1186/s13020-023-00857-y.
6. Wang, Y.; Choi, H.K.; Brinckmann, J.A.; Jiang, X.; Huang, L. Chemical analysis of Panax quinquefolius (North American ginseng): A review. *J Chromatogr A* **2015**, *1426*, 1-15, doi:10.1016/j.chroma.2015.11.012.
7. Wei, G.; Zhang, G.; Li, M.; Zheng, Y.; Zheng, W.; Wang, B.; Zhang, Z.; Zhang, X.; Huang, Z.; Wei, T.; et al. Panax notoginseng: panoramagram of phytochemical and pharmacological properties, biosynthesis, and regulation and production of ginsenosides. *Hortic Res* **2024**, *11*, uhae170, doi:10.1093/hr/uhae170.
8. Zeng, T.X.; Pei, J.; Miao, Y.J.; Zheng, Y.; Gu, S.J.; Zhao, L.; Huang, L.F. Current Status and Research Trends of Panax Between 1900-2019: A Bibliometric Analysis. *Chin J Integr Med* **2022**, *28*, 547-553, doi:10.1007/s11655-021-3315-8.
9. Qiu, Z.; Zhao, X.; Liu, M.; Liu, Y.; Sun, L.; Ren, X.; Deng, Y. Identification of the Origin, Authenticity and Quality of Panax Japonicus Based on a Multistrategy Platform. *Comb Chem High Throughput Screen* **2023**, *26*, 1375-1384, doi:10.2174/1386207325666220822102014.
10. Jinbiao, L.; Xinyue, Z.; Shenshen, Y.; Shuo, W.; Chengcheng, L.; Bin, Y.; Yubo, L.; Ting, C. Rapid Identification of Characteristic Chemical Constituents of Panax ginseng, Panax quinquefolius, and Panax japonicus Using UPLC-Q-TOF/MS. *J Anal Methods Chem* **2022**, *2022*, 6463770, doi:10.1155/2022/6463770.
11. Wu, W.R.; Cheng, C.S.; Cheng, Q.Q.; Lao, C.C.; Cui, H.; Tang, Z.Y.; Ouyang, Y.; Liu, L.; Zhou, H. Novel SNP markers on ginsenosides biosynthesis functional gene for authentication of ginseng herbs and commercial products. *Chin J Nat Med* **2020**, *18*, 770-778, doi:10.1016/s1875-5364(20)60017-6.
12. Ichim, M.C.; de Boer, H.J. A Review of Authenticity and Authentication of Commercial Ginseng Herbal Medicines and Food Supplements. *Front Pharmacol* **2020**, *11*, 612071, doi:10.3389/fphar.2020.612071.
13. Xia, P.; Bai, Z.; Liang, T.; Yang, D.; Liang, Z.; Yan, X.; Liu, Y. High-performance liquid chromatography based chemical fingerprint analysis and chemometric approaches for the identification and distinction of three endangered Panax plants in Southeast Asia. *J Sep Sci* **2016**, *39*, 3880-3888, doi:10.1002/jssc.201600460.
14. Yang, L.; Jiang, H.; Wang, S.; Hou, A.; Man, W.; Zhang, J.; Guo, X.; Yang, B.; Kuang, H.; Wang, Q. Discovering the Major Antitussive, Expectorant, and Anti-Inflammatory Bioactive Constituents in Tussilago Farfara L. Based on the Spectrum-Effect Relationship Combined with Chemometrics. *Molecules* **2020**, *25*, doi:10.3390/molecules25030620.
15. Zhou, X.; Liu, H.; Zhang, M.; Li, C.; Li, G. Spectrum-effect relationship between UPLC fingerprints and anti-lung cancer effect of Panax ginseng. *Phytochem Anal* **2021**, *32*, 339-346, doi:10.1002/pca.2980.
16. Yang, W.Z.; Ye, M.; Qiao, X.; Liu, C.F.; Miao, W.J.; Bo, T.; Tao, H.Y.; Guo, D.A. A strategy for efficient discovery of new natural compounds by integrating orthogonal column chromatography and liquid chromatography/mass spectrometry analysis: Its application in Panax ginseng, Panax quinquefolium and Panax notoginseng to characterize 437 potential new ginsenosides. *Anal Chim Acta* **2012**, *739*, 56-66, doi:10.1016/j.aca.2012.06.017.
17. Souza, A.S.; Bezerra, M.A.; Cerqueira, U.; Rodrigues, C.J.O.; Santos, B.C.; Novaes, C.G.; Almeida, E.R.V. An introductory review on the application of principal component analysis in the data exploration of the chemical analysis of food samples. *Food Sci Biotechnol* **2024**, *33*, 1323-1336, doi:10.1007/s10068-023-01509-5.
18. Peng, C.; Zhu, Y.; Yan, F.; Su, Y.; Zhu, Y.; Zhang, Z.; Zuo, C.; Wu, H.; Zhang, Y.; Kan, J.; Peng, D. The difference of origin and extraction method significantly affects the intrinsic quality of licorice: A new method for quality evaluation of homologous materials of medicine and food. *Food Chem* **2021**, *340*, 127907, doi:10.1016/j.foodchem.2020.127907.
19. Han, J.; Xu, K.; Yan, Q.; Sui, W.; Zhang, H.; Wang, S.; Zhang, Z.; Wei, Z.; Han, F. Qualitative and quantitative evaluation of Flos Puerariae by using chemical fingerprint in combination with chemometrics method. *J Pharm Anal* **2022**, *12*, 489-499, doi:10.1016/j.jpha.2021.09.003.
20. Li, L.; Wang, Y.; Xiu, Y.; Liu, S. Chemical Differentiation and Quantitative Analysis of Different Types of Panax Genus Stem-Leaf Based on a UPLC-Q-Exactive Orbitrap/MS Combined with Multivariate Statistical Analysis Approach. *J Anal Methods Chem* **2018**, *2018*, 9598672,

doi:10.1155/2018/9598672.

21. Huang, B.M.; Zha, Q.L.; Chen, T.B.; Xiao, S.Y.; Xie, Y.; Luo, P.; Wang, Y.P.; Liu, L.; Zhou, H. Discovery of markers for discriminating the age of cultivated ginseng by using UHPLC-QTOF/MS coupled with OPLS-DA. *Phytomedicine* **2018**, *45*, 8-17, doi:10.1016/j.phymed.2018.03.011.
22. Sun, Y.; Fu, X.; Qu, Y.; Chen, L.; Liu, X.; He, Z.; Xu, J.; Yang, J.; Ma, W.; Li, J.; et al. Characterization of Ginsenosides from the Root of Panax ginseng by Integrating Untargeted Metabolites Using UPLC-Triple TOF-MS. *Molecules* **2023**, *28*, doi:10.3390/molecules28052068.

Figures

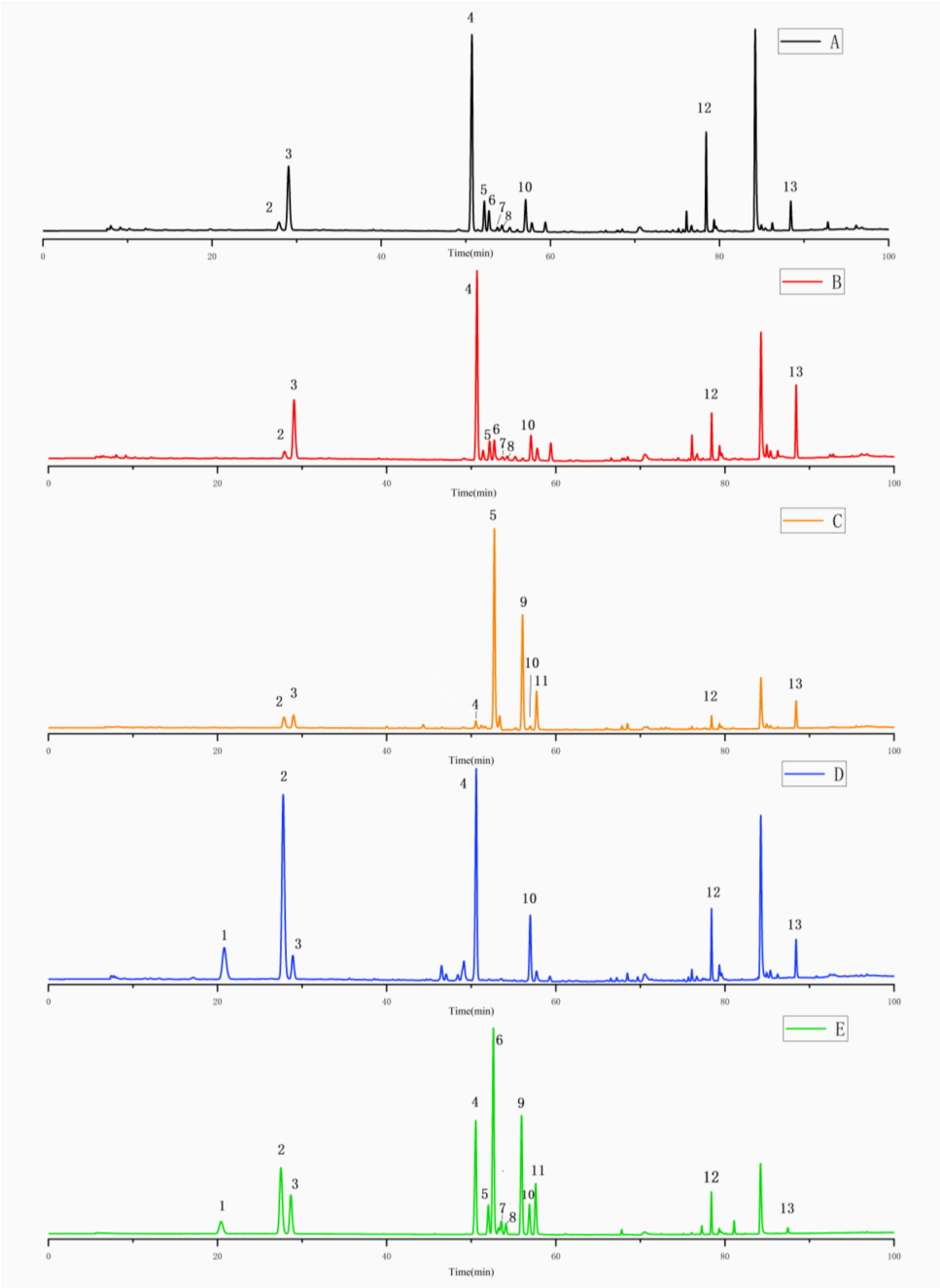

Fig. 1 The HPLC chromatograms of RS(A), XYS(B), BSQ(C), SQ(D) and Mixed standards sol ution(E), 1: notoginsenoside R1, 2: ginsenoside Rg1, 3: ginsenoside Re, 4: ginsenoside Rb1, 5: ginsenoside Ro, 6: ginsenoside Rc, 7: ginsenoside Rb2, 8: ginsenoside Rb3, 9: chikusetsusaponi n IV, 10: ginsenoside Rd, 11: chikusetsusaponin IVa, 12: panaxydol and 13: panaxynol.

Figure 1

See image above for figure legend

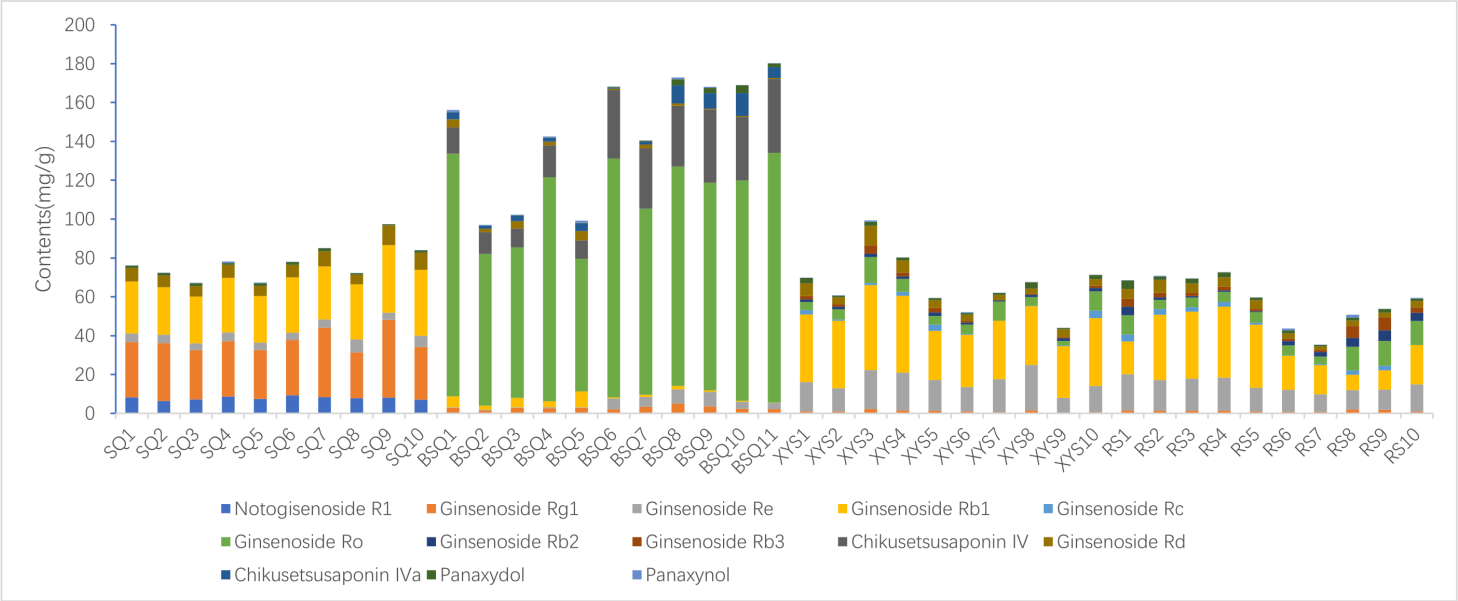

Fig. 2 Content chromatograms of the four medicinal materials.

Figure 2

See image above for figure legend

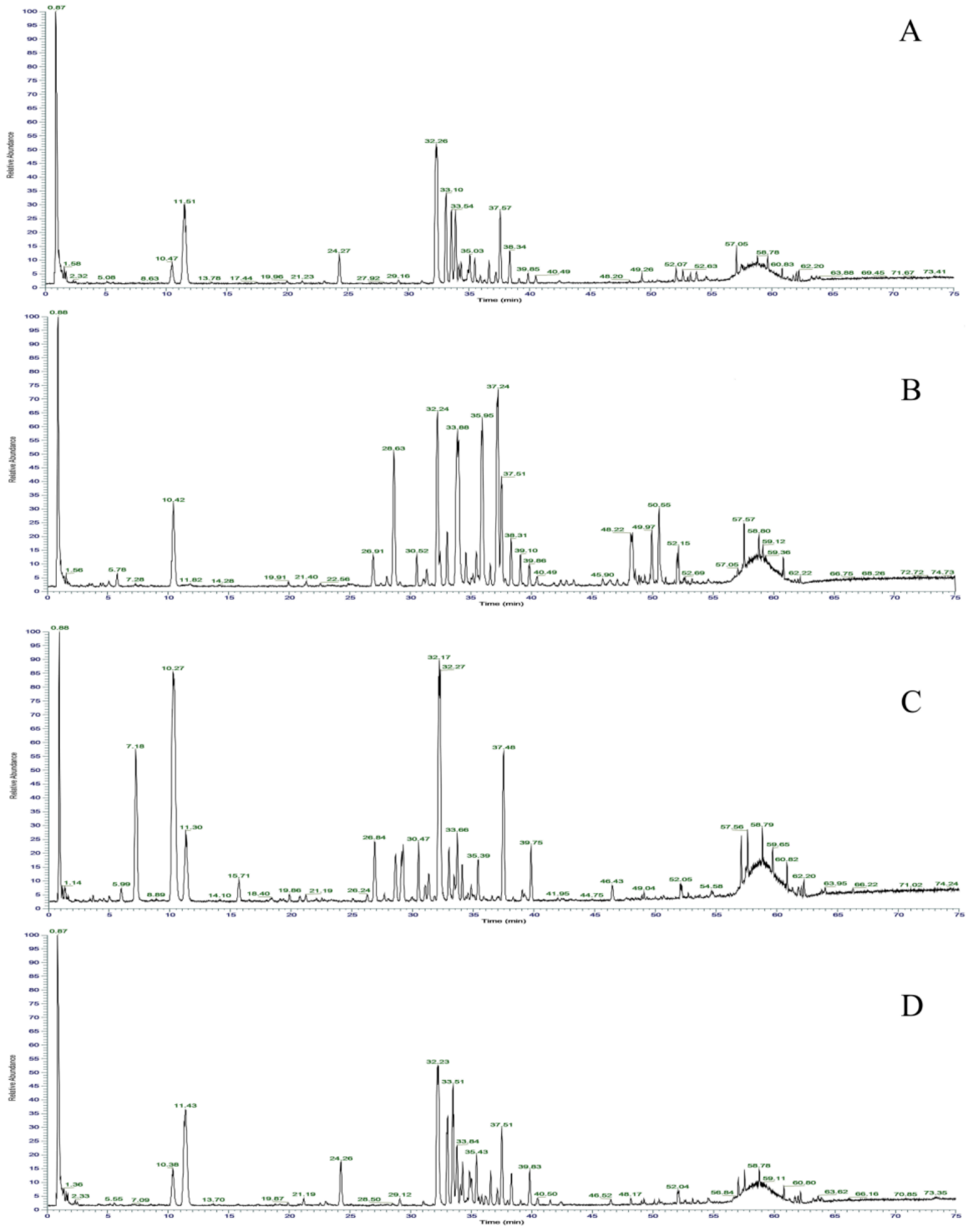

Fig. 3 Negative total ion chromatograms of RS(A), BSQ(B), SQ(C), and XYS(D).

Figure 3

See image above for figure legend

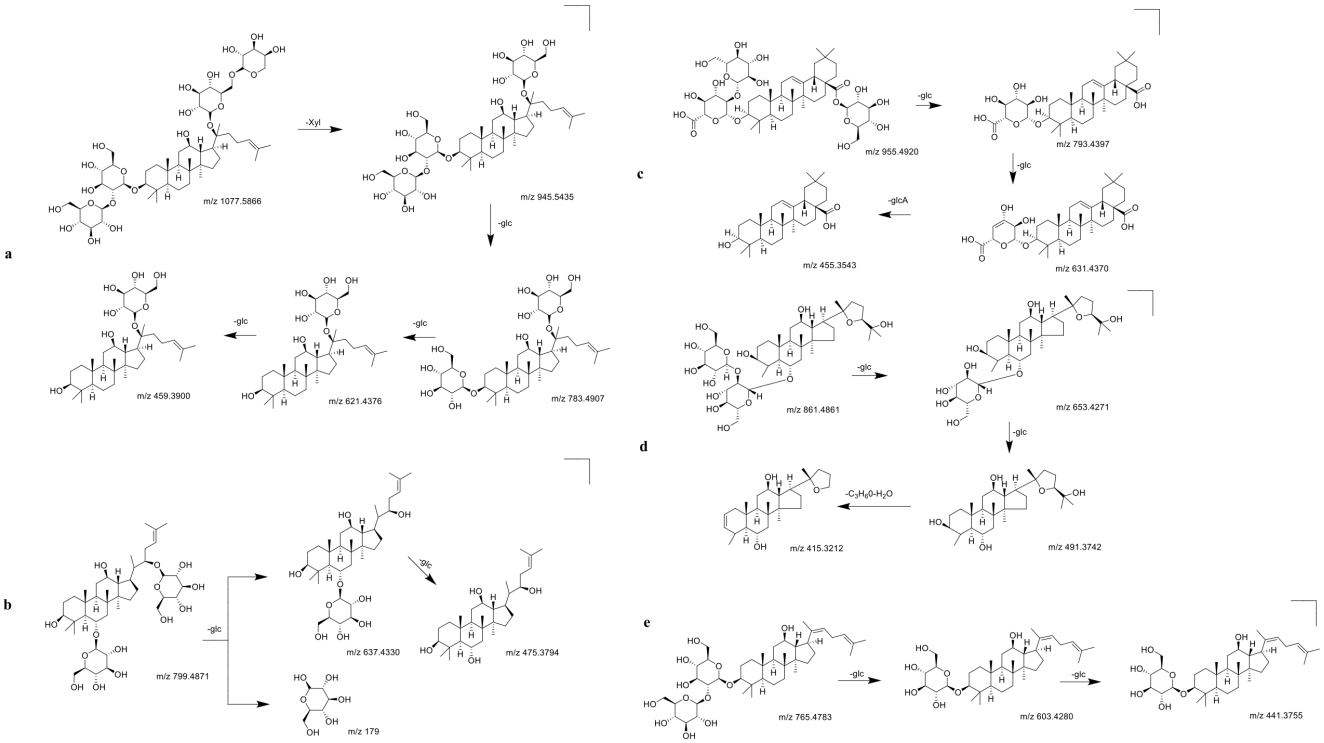

Fig. 4 Fragmention pathways of of various components in Four Panax species.a: Protopanaxadiol,b: Protopanaxatriol,c: Oleanolic acid,d: Octillol,e: C17 side-chain varied.

Figure 4

See image above for figure legend

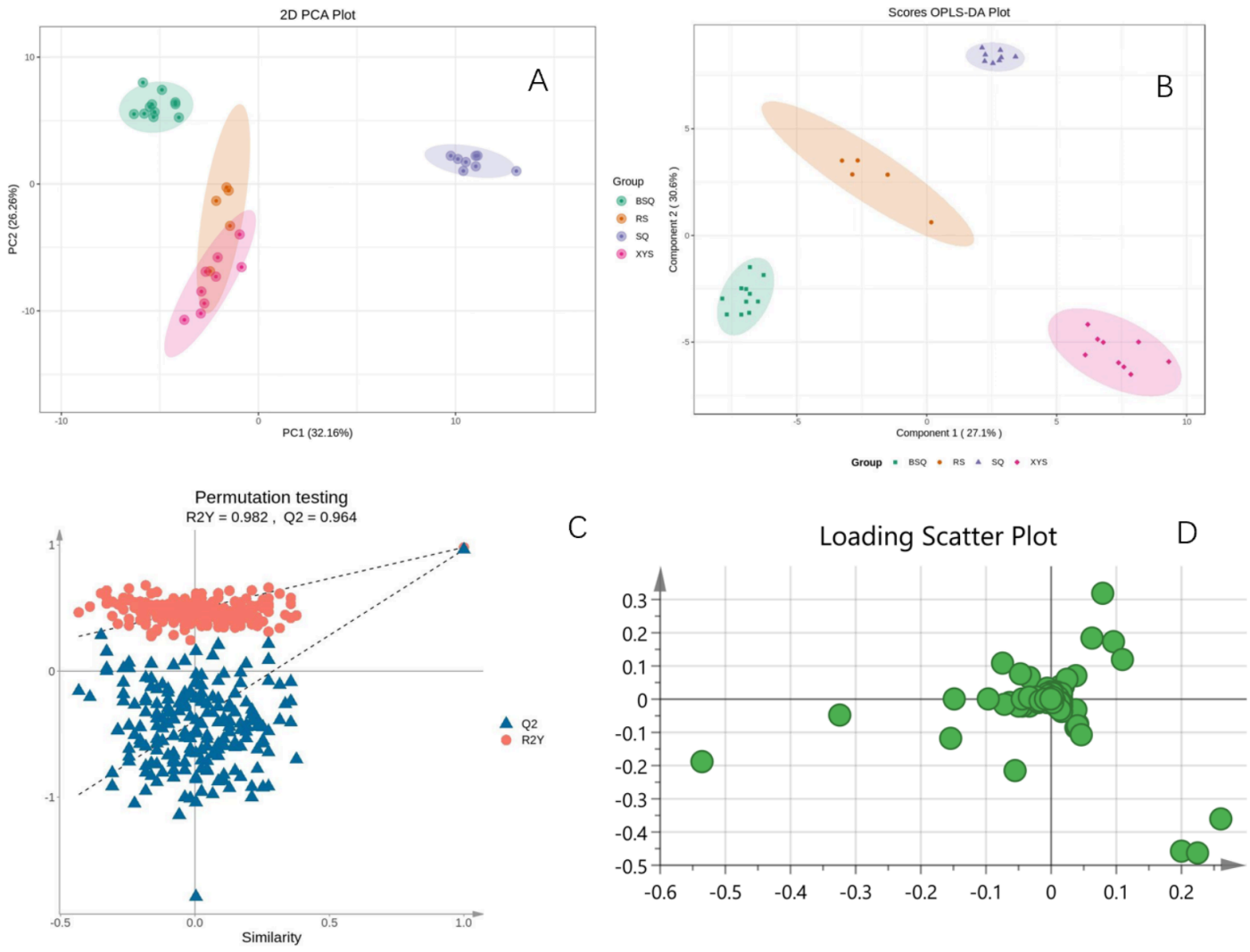

Fig. 5 PCA score plot (A), OPLS-DA score plot (B), Permutation test plot of the OPLS-DA (C),and Loading Scatter Plot (D).

Figure 5

See image above for figure legend

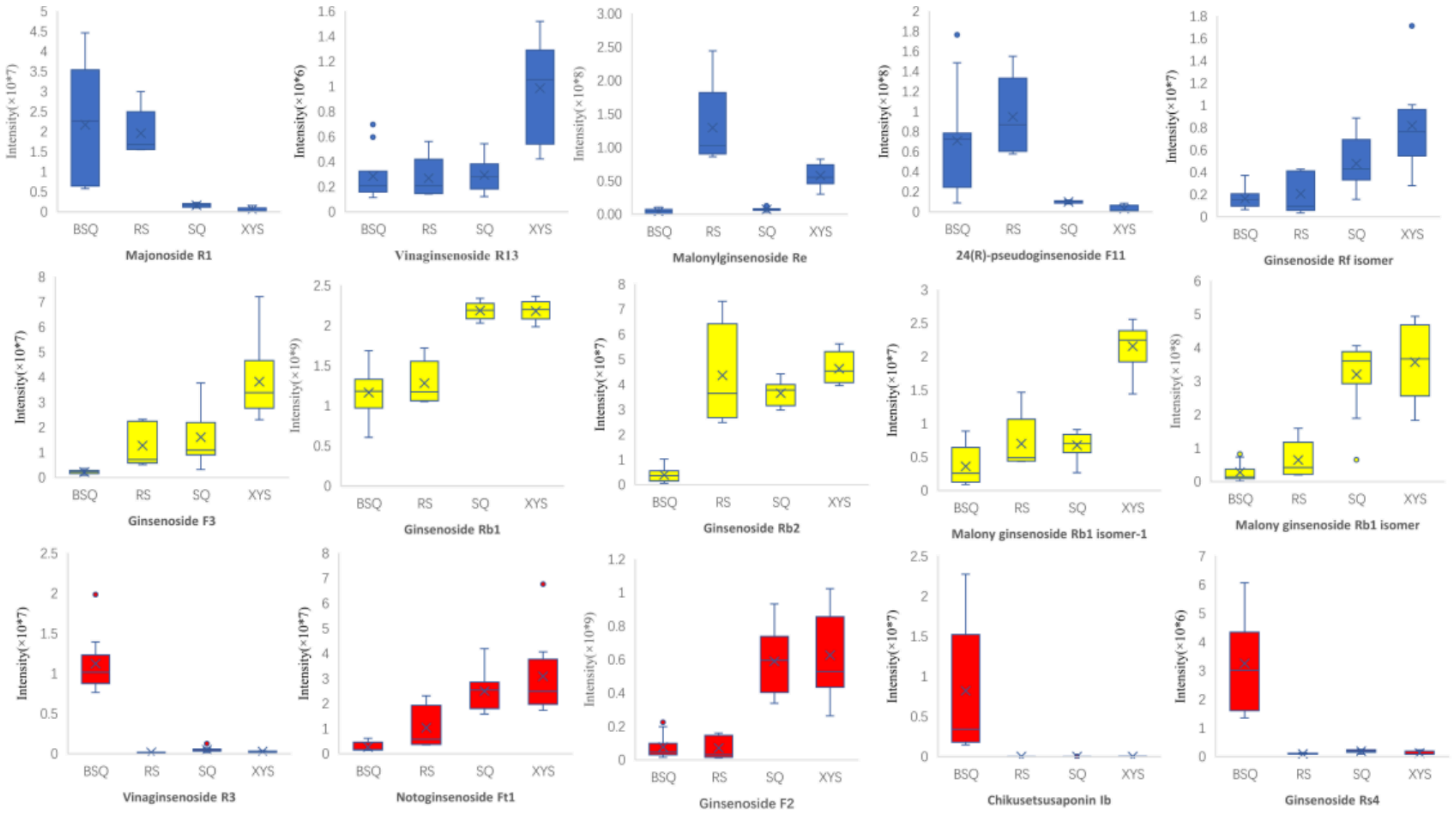

Fig. 6 Box plots illustrating the distribution of the relative abundances of the 15 significantly differential compounds screened by OPLS-DA (VIP > 1.5) across four Panax species.

Figure 6

See image above for figure legend

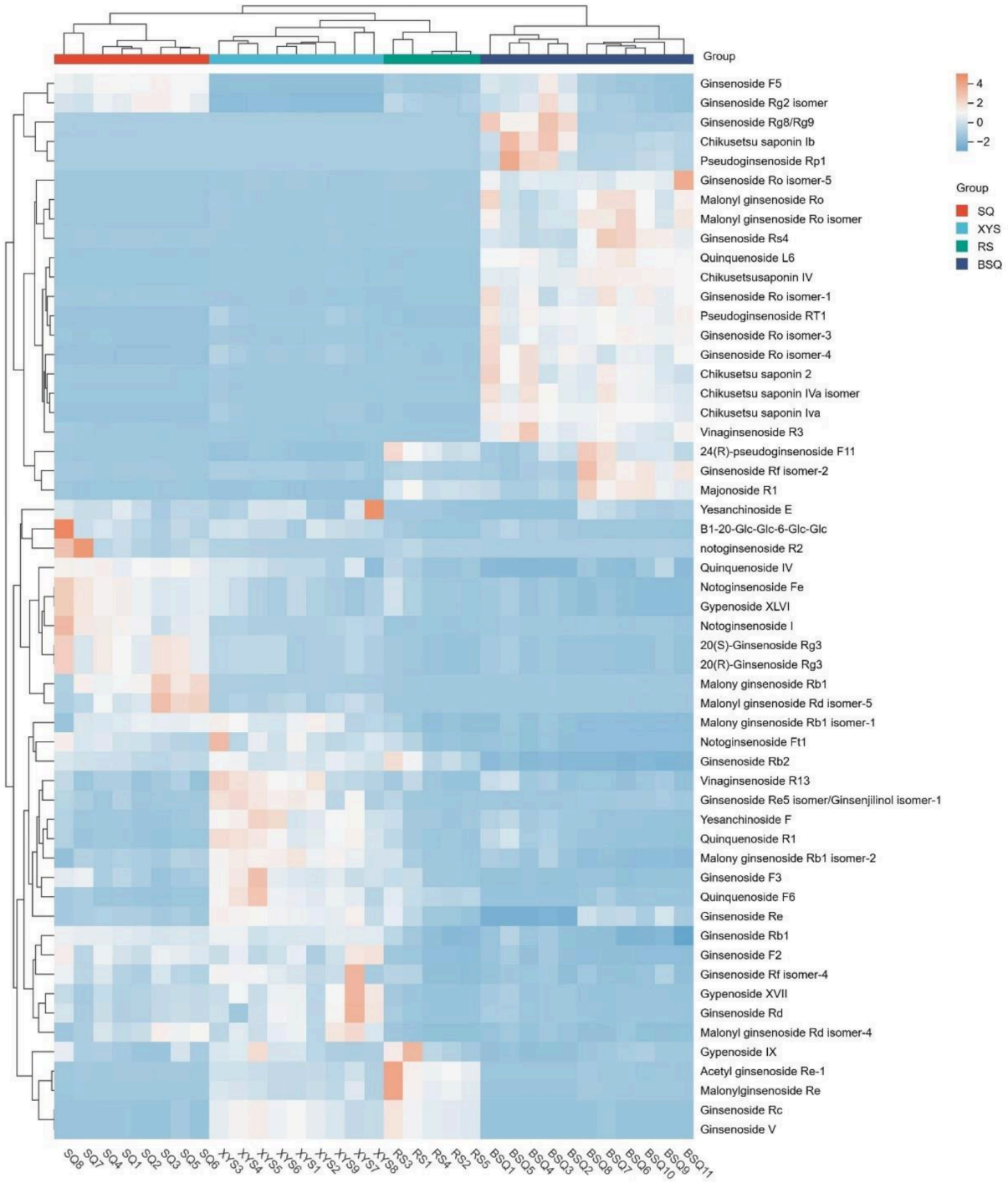

Fig. 7 Heatmap of four Panax species.

Figure 7

See image above for figure legend

Supplementary Files

This is a list of supplementary files associated with this preprint. Click to download.

- SupplementaryMaterials.docx